Development of ultrafast computed tomography of highly transient fuel sprays

Xin Liu, Jinyuan Liu, Xuefa Li, Seong-Kyun Cheong, Deming Shu, Jin Wang*
Argonne National Laboratory, 9700 South Cass Avenue, Argonne, IL, USA 60439

Mark W. Tate[a], Alper Ercan[a], Daniel R. Schuette[a], Matt J. Renzi[a], Arthur Woll[b], Sol M. Gruner[a, b]
[a]Department of Physics and [b]Cornell High Energy Synchrotron Source, Cornell University, Ithaca, NY, USA 14853

ABSTRACT

The detailed analysis of the fuel sprays has been well recognized as an important step for optimizing the operation of internal-combustion engines to improve efficiency and reduce emissions. However, the structure and dynamics of highly transient fuel sprays have never been visualized or reconstructed in three dimensions (3D) previously due to numerous technical difficulties. By using an ultrafast x-ray detector and intense monochromatic x-ray beams from synchrotron radiation, the fine structures and dynamics of 1-ms direct-injection gasoline fuel sprays were elucidated for the first time by a newly developed, ultrafast computed microtomography technique. Due to the time-resolved nature and the intensive data analysis, the Fourier transform algorithm was used to achieve an efficient reconstruction process. The temporal and spatial resolutions of the current measurement are 5.1 μs and 150 μm, respectively. Many features associated with the transient liquid flows are readily observable in the reconstructed spray. Furthermore, an accurate 3D fuel density distribution was obtained as the result of the computed tomography in a time-resolved manner. These results not only reveal the characteristics of automotive fuel sprays with unprecedented details, but will also facilitate realistic computational fluid dynamic simulations in highly transient, multiphase systems.

Keywords: fuel spray, synchrotron X-ray, tomography

1. INTRODUCTION

High-pressure, high-speed liquid sprays are an essential technology for many industrial and consumer applications, such as automotive fuel injection systems. As the worldwide demand for energy grows rapidly, the technologies capable of improving fuel efficiency and reducing emissions should play an essential role in the design of the new-generation automotive internal combustion engines.[1] Among these is gasoline direct-injection (GDI) technology, which has been the subject of research and development for a long time in the automotive industry. In a combustion system employing GDI, the fuel is directly injected into the combustion chamber instead of the air-intake port. Due to the ability to precisely control the injection rate, timing, and combustion of the fuel, the fuel efficiency can be greatly improved. Therefore, detailed analyses of the fuel sprays in the GDI systems become extremely important for optimizing their operation.[1,2] Traditionally, quantitative fuel spray characterization has been difficult because it requires analysis of submillimeter-scale structures with microsecond time resolution in a complex multiphase flow. Despite significant advances in laser diagnostics in the past, the region close to the nozzle still has not yielded the desired quantitative information due to the optical multiple scattering from the fuel droplets.[3-5] Recently, a new nonintrusive, quantitative, and highly time-resolved technique to characterize the dense part of fuel sprays has been developed based on monochromatic X-radiography.[6-9] Such a technique takes advantage of high intensity and high monochromaticity of the synchrotron radiation X-rays, which makes accurate quantitative measurement of highly transient (with a duration of ~ 1 ms) fuel sprays within a time-resolved manner. Some interesting phenomena are observed, such as shockwaves

* wangj@aps.anl.gov

generated by high-pressure diesel fuel sprays[7] and severe axial asymmetry in GDI sprays from symmetric annular nozzles.[8]

Even with the X-radiography technique, however, the highly transient fuel sprays have never been visualized or reconstructed in a true three-dimensional (3D) manner. The intent to qualitatively visualize and measure fuel spray characteristics such as internal structure, density distribution, and flow dynamics, requires the development of an ultrafast X-tomography technique capable of capturing the transient nature of the sprays.

Tomography, whether it is through transmission or emission, has been an important method in medical diagnosis since its invention. The basic principle of the transmission tomography, which we employ for our fuel spray experiment, is reconstructing a planar object (slice) from the values of its line integrals from different viewing angles. Then, the 3D object can be built by stacking up all the reconstructed slices.[10] Clearly, the resolution of reconstruction depends on the number of line integrals and the number of viewing angles. In the late 1980s, new-generation tomography with micrometer resolution and time-resolved capability was developed owing to the advent of synchrotron radiation.[11-14] With the availability of fast direct X-ray area imagers, it has become possible to apply tomography techniques to elucidate the internal structure of the fuel sprays in an ultrafast manner. Here, we describe a new transmission microtomography system developed at the Advanced Photon Source (APS), coupled with a state-of-the-art two dimensional (2D) X-ray pixel array detector (PAD) developed at Cornell University,[15-17] to image and quantitatively reconstruct GDI hollow-cone sprays.

2. EXPERIMENTAL METHODS

The fuel spray tomography experiments are performed at the D-1 beamline of the Cornell High Energy Synchrotron Source (CHESS). The schematic experimental setup is shown in Fig. 1. The X-ray beam produced by synchrotron radiation is monochromatized to 6.0 keV using a double-multilayer monochromator. This X-ray energy is optimal for probing the fuel, a blend of a calibration fluid and a cerium-containing fuel additive. The calibration fluid (Viscor 16-A) is a simulated fuel with properties similar to gasoline fuel with precisely controlled viscosity and specific gravity specifications. The additive, originally developed for combustion emission reduction, was used to enhance the fuel spray contrast in the X-ray transmission measurement. The monochromatized X-ray beam is collimated to 15 mm (H) x 2 mm (V) by a set of slits as shown in Fig. 1.

The next important component in the tomography setup is a cylindrical spray chamber that is made of stainless steel with 11-cm inner diameter and 21-cm height. This injection chamber is intended to provide environment enclosure for the fuel sprays. As shown in Fig. 1, there are two identical X-ray transparent windows situated symmetrically on the chamber with a 120^{o} X-ray viewing angle. The windows are 6.5 cm high and are covered with polymer thin films. The injection nozzle is mounted on the top of the chamber as shown in Fig. 1. The nozzle has an outwardly opening pintle and an annular orifice with a diameter of 1.9 mm. The injection pressure is about 7 MPa and the nominal duration of the spray is 1 ms. Also fit to the chamber are two inlets and one outlet for flowing nitrogen gas through the chamber to scavenge the fuel vapor. On the side of the chamber, there is also a fuel drain line. The environment in the spray chamber is maintained at one atmospheric pressure and at room temperature (27-30°C in the D-1 radiation enclosure).

The spray chamber is designed to rotate and to translate in precise steps while the X-ray source and the detector are stationary. In this system, we use a horizontal rotational stage and a vertical translational stage to rotate the spray chamber and to select the slice to be imaged in the vertical direction. The minimum rotation angle is 0.0025^{o}, and the minimum step size for the translation stage is 1.27 μm. In the experiment, the parallel X-ray beams penetrate the spray at a given view angle θ, and after completion of the scans in temporal steps, the injector nozzle rotates a small angle $\Delta\theta$ and the temporal scans are repeated. This process is continued until the completion of 180^{o} rotation.

The rotating injection nozzle in this tomography system poses a rigorous requirement of alignment. First, the rotation axis and the X-ray beam should be orthogonal, which is achieved by adjusting the optical table supporting the spray chamber. Second, it is essential to ensure the coincidence of the rotation axis and the center of the injection nozzle. The alignment is completed by adjusting the X-Y translation stages mounted under the spray chamber (not shown in the schematic). All the rotational and translational stages are motorized.

Another key component in the setup is the ultrafast X-ray framing detector – PAD. The pixel size of the PAD is 150 x 150 μm^2. The single imaging area is 92 (H) x 31 (V) pixels limited by the X-ray beam size. The complete imaging area is built up by shifting the position of the injector relative to the beam and the PAD. During the experiment, the spray is fired at 1.15 Hz and a series of frames is taken at various delay times. The exposure time per frame is set to 5.13 μs (twice the CHESS synchrotron period) with an interval between frames of 15.38 μs. Each image is obtained by averaging 20 fuel-injection cycles. The total acquisition time for each angle is about 5 minutes.

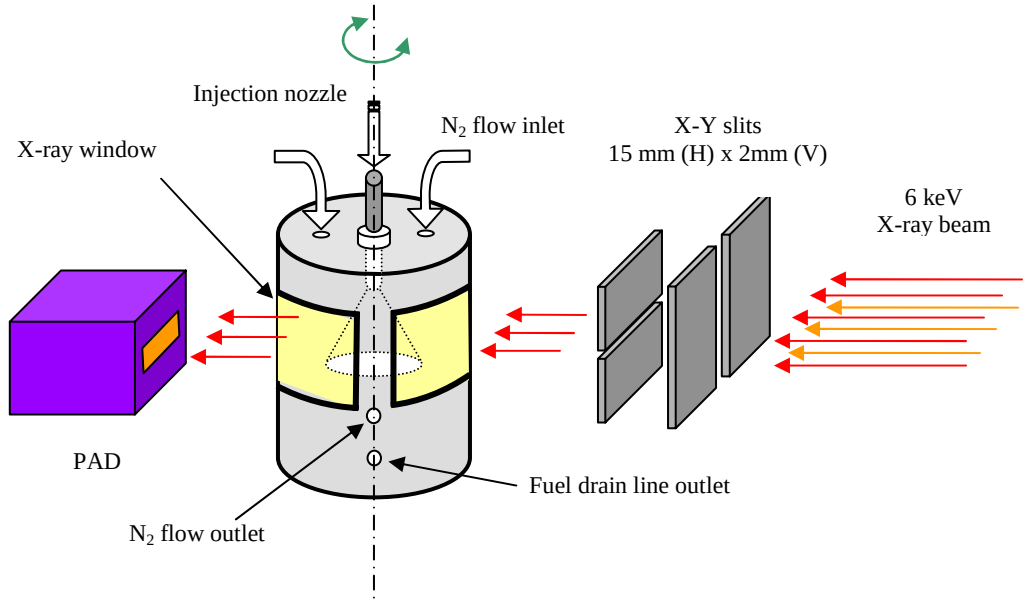

Fig. 1. Schematic of the experimental setup.

3. RECONSTRUCTION METHODS

The mathematical description of the fuel spray tomography is built upon the experimental geometry described in Fig. 1. Consider a parallel X-ray beam transmitting an object (the hollow cone spray in this case) as shown in Fig. 2. The function $f(x, y)$ represents the linear attenuation coefficients where (x, y) are the Cartesian coordinates fixed on one slice of the spray. A set of laboratory coordinates (r, s) are also defined as shown in Fig. 2 while (x, y) can rotate about the origin. With a rotational angle θ, The two coordinate systems can be transformed by

$$\begin{bmatrix} x \\ y \end{bmatrix} = \begin{bmatrix} \cos\theta & \sin\theta \\ -\sin\theta & \cos\theta \end{bmatrix} \begin{bmatrix} r \\ s \end{bmatrix}. \tag{1}$$

Since monochromatic X-ray beams are used, the transmitted X-ray intensity profile I as a function of r at given angle θ is simply described by

$$\begin{aligned} I(r,\theta) &= I_0 \exp[-\int_s f(x,y)ds] \\ &= I_0 \exp[-\int_s f(r\cos\theta + s\sin\theta, -r\sin\theta + s\cos\theta)ds], \end{aligned} \tag{2}$$

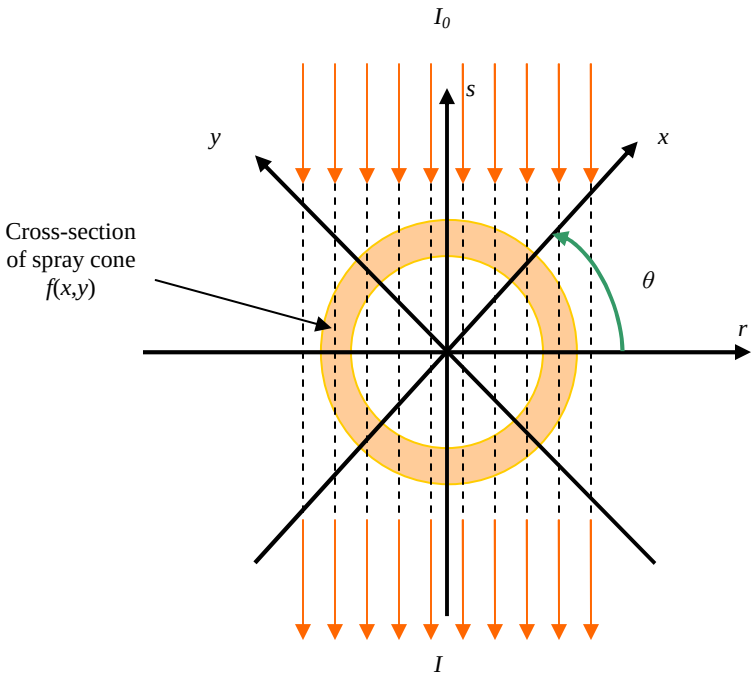

Fig. 2. Definition of spray and laboratory coordinate systems.

where I_0 is the incident X-ray beam intensity and ds is the spatial interval along the beam path. The sinogram $p(r, \theta)$ in polar coordinates (r, θ) is defined by

$$\begin{aligned} p(r,\theta) &= -\ln\frac{I(r,\theta)}{I_0} \\ &= \int_s f(r\cos\theta+\sin\theta,-r\sin\theta+s\cos\theta)ds, \end{aligned} \tag{3}$$

which is the mathematical description of the imaging data set recorded by the PAD.

With the sinogram, we can reconstruct $f(x, y)$ by several numerical methods based on filtered backprojection (FBP), algebraic reconstruction, and the Fourier transform algorithm. The algebraic reconstruction method is the slowest algorithm of the three methods, but it can be used when the tomographic data are not collected with uniform angular intervals. The results given by the FBP method and Fourier transform method are very close for our case, but the latter has proven to be the most efficient algorithm. Thus, we choose the Fourier transform algorithm as our reconstruction method. With the well-known central slice theorem (CST), one can reconstruct $f(x, y)$ through the Fourier transform and the inverse Fourier transform as shown in equation (4):

$$f(x,y) = F^{-1}\{F[f(x,y)]\} = F^{-1}\{F[p(r,\theta)]\}, \tag{4}$$

where F and F^{-1} are the Fourier transform and the inverse Fourier transform, respectively. The normalized linear attenuation in one pixel is obtained by

$$f_N(x,y) = \frac{f(x,y)}{\Delta s}. \tag{5}$$

The mass density distribution $\rho(x, y)$ is simply derived by

$$\rho(x,y) = \frac{f_N(x,y)}{\mu_M}, \tag{6}$$

where μ_M is the mass attenuation coefficient of the fuel, which is evaluated through a calibration procedure.[6]

The next experimental parameter that needs to be determined is the minimum number of view angles. This can be achieved by considering the reconstruction resolution and the limited data collection time. The number of view angles is also dependent on the size of the viewing area. The larger viewing area needs more view angles. By equating the radial resolution and the worst-case azimuthal resolution, the minimum number of view angles required is estimated by,[10]

$$N_v = \frac{\pi}{2} N_p, \tag{7}$$

where N_v is the number of view angles and N_p is the number of data pixels. For example, there are 92 pixels horizontally to record the projections in the PAD, resulting in a minimum N_v of 145. In the actual experiment, 180 view angles are used.

4. RESULTS AND DISCUSSION

The tomographic images of the GDI sprays taken by PAD at selected projection angles are shown in Fig. 3. These images show the progression of the spray with unprecedented details. "sac", streaks, and asymmetry are readily observed. As shown in Fig. 4, the fuel density distribution of a single slice is reconstructed at different locations. Although sprays come out of an annular orifice, the cross section of the spray cone is not perfectly circular and the density distribution is far from axially symmetric. The averaged fuel density falls off rapidly as the spray progresses forward. Believed due to fuel atomization, the maximum density of 80 μg/mm^3 at only 1.5 mm away from the nozzle is much lower than the liquid density of the test fuel blend (857.7 μg/mm^3).

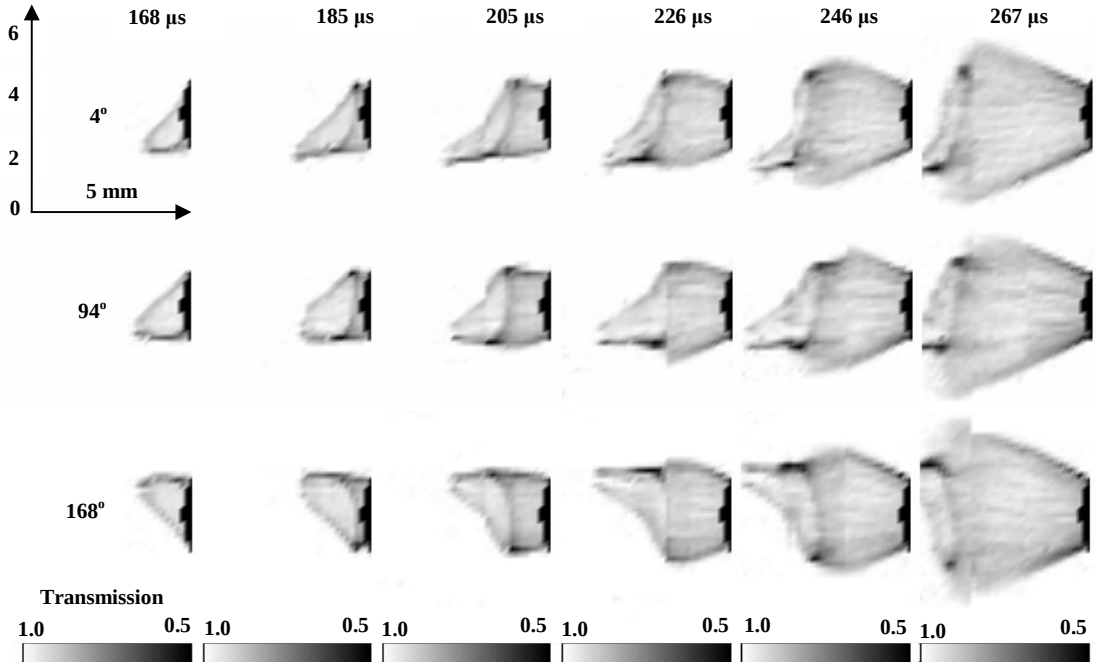

Fig. 3. Tomographic images of hollow-cone GDI fuel sprays at projection angles of 4°, 94°, and 168° and at various time instances after the start of the injection.

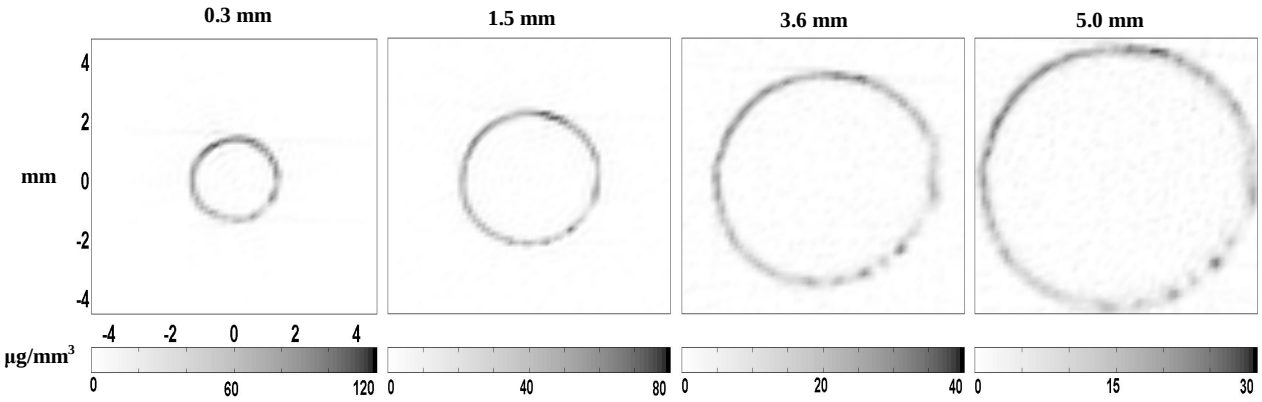

Fig. 4. Reconstructed fuel density distribution at 820 μs at different locations from nozzle.

Figure 5 shows a time series of the cross-sectional fuel-density distribution at 3.5 mm from the nozzle. These reconstructed cross sections indicate the arrival of the spray leading edge (267 μs), steady hollow cone (820 and 1148 μs), and the arrival of the trailing edge (1271 μs), respectively. These results validate the results shown in reference 8, where a model-dependent reconstruction on a similar experiment is performed. Clearly demonstrated in this measurement is the degree of the spray details that can not be obtained by the model-dependent reconstruction.

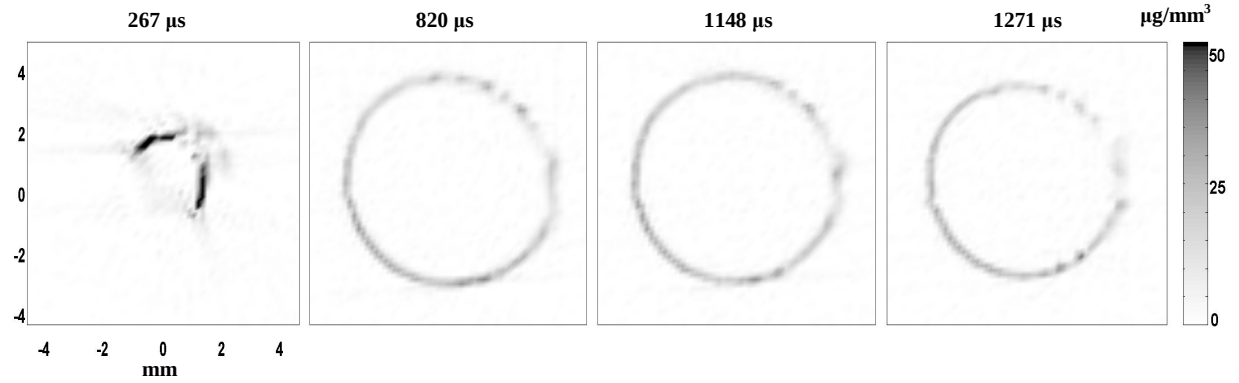

Fig. 5. Fuel density distribution at 3.5 mm from the nozzle at different times.

The results shown above certainly indicate a progress toward revealing the nature of fuel sprays at the near-nozzle region if the fidelity of the reconstruction can be verified. One method to prove the validity of spray reconstructions is by the comparing the sinogram measured experimentally and the numerical projection of the reconstructed spray slice. Figure 6 shows the comparison at several view angles at 3.5 mm from the nozzle and 636 μs after the start of the injection. The extremely good agreement between the two data sets is demonstrated.

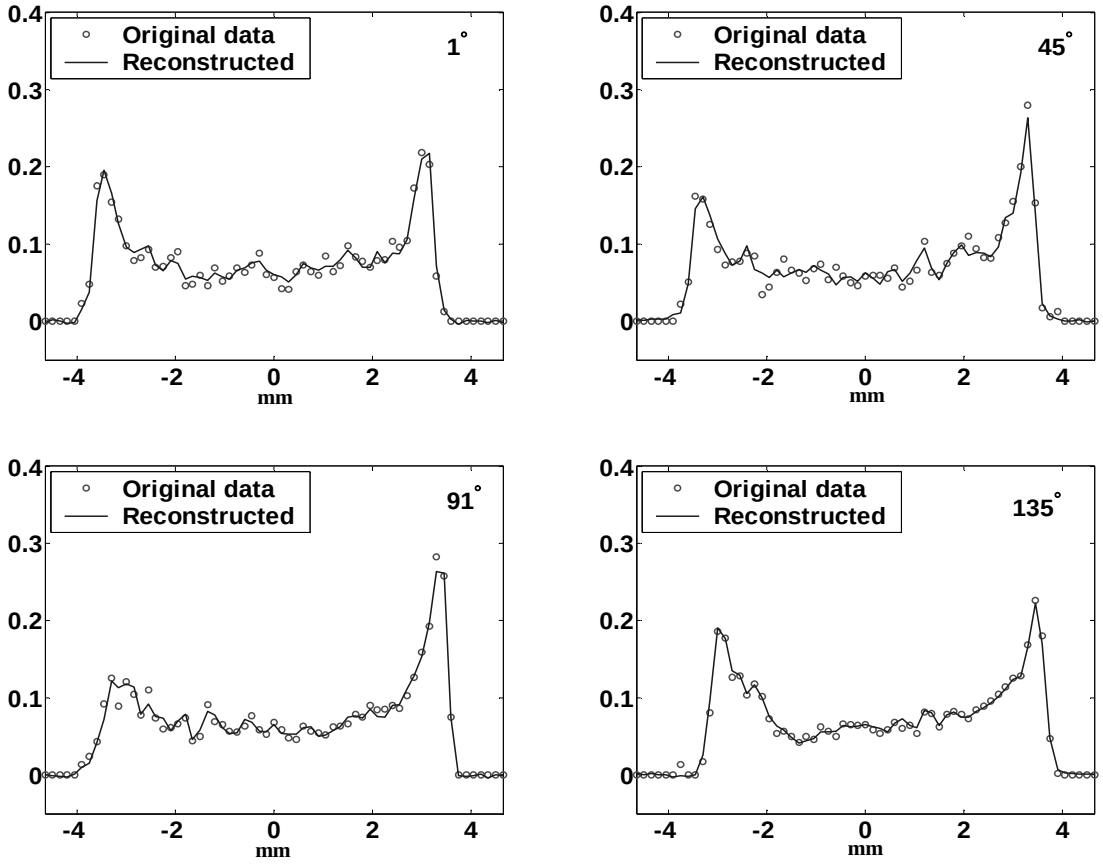

Fig. 6. Comparison between original data and data obtained by scanning the reconstructed spray at 3.5 mm from the nozzle and 636 μs after the start of the injection.

5. CONCLUSION

An ultrafast tomography system has been developed for the first time to study the highly transient GDI fuel sprays. The time evolution of the sprays is directly imaged and the near-nozzle spray structure has been fully reconstructed quantitatively with submillimeter spatial resolution and 5-μs temporal resolution. The validity of the reconstruction has also been demonstrated. We believe these results will further the understanding of the dynamics and structures of the fuel spray. Furthermore, detailed 3D spray distribution will facilitate development of realistic computational fluid dynamic simulations in complex multiphase flows. We also believe that the methodology demonstrated here is also a sensitive probe and diagnostic tool for investigating other highly transient phenomena.

ACKNOWLEDGEMENTS

The authors would like to thank Christopher F. Powell for his technical support, Francesco De Carlo for his helpful discussion. The work is supported by the U.S. Department of Energy under Contract W-31-109-ENG-38 through an Argonne National Laboratory LDRD grant. The authors are also thank the staff at CHESS, funded by the U.S. National Science Foundation (NSF) and the U.S. National Institute of General Medical Sciences via NSF under award DMR-9713424. PAD detector development was funded by DOE grants DE-FG-0297ER14805 and DE-FG-0297ER62443.

REFERENCES

1. Cohn, D. R. and J. B. Heywood, "Energy Issues for Vehicles: R&D, Carbon Sequestration, Fuel Conversion," *Physics Today*, Vol. 55, 2002, 12-13.
2. Zhao, F., M.-C. Lai and D. L. Harrington, "Automotive Spark-ignited Direct-Injection Gasoline Engines," *Progress in Energy and Combustion Science*, Vol. 25, 1999, 437-562.
3. Adrian, R. J., "Particle-Imaging Techniques for Experimental Fluid Mechanics," *Ann. Rev. Fluid Mechanics*, Vol. 23, 1991, 261-304.
4. Coil, M. A. and P. V. Farrell, "Investigation of Diesel Sprays Using Diffraction-Based Droplet Sizing," *Society of Automotive Engineers*, Technical Paper SAE 950458, 1995.
5. Sick, V. and B. Stojkovic, "Attenuation Effects on Imaging Diagnostics of Hollow-cone Sprays," *Applied Optics*, Vol. 40, No. 15, 2001, 2435-2442.
6. Powell, C. F. et al., "Time-Resolved Measurements of Supersonic Fuel Sprays using Synchrotron X-rays," *J. Synchrotron Rad.*, Vol. 7, 2000, 356-360.
7. MacPhee, A. G. et al., "X-ray Imaging of Shock Waves Generated by High-Pressure Fuel Sprays," *Science*, Vol. 295, 2002, 1261-1263.
8. Cai, W. et al., "Quantitative Analysis of Highly Transient Fuel Sprays by Time-Resolved X-Radiography," *Applied Physics Letters*, Vol. 83, No. 8, 2003, 1671-1673.
9. Cheong, S.-K. et al., "Effects of Ambient Pressure on Dynamics of Near-Nozzle Diesel Sprays Studied by Ultrafast X-Radiography," *Society of Automotive Engineers*, Technical Paper SAE 012026, 2004.
10. Kak, Avinash C. and Malcolm Slaney, *Principles of Computerized Tomographic Imaging*, IEEE Press, New York, 1999.
11. Grodzins, L., "Optimum Energies for X-ray Transmission Tomography of Small Samples-Applications of Synchrotron Radiation to Computerized Tomography I," *Nuclear Instruments and Methods*, Vol. 206, 1983, 541-545.
12. Flannery, B. P. et al., "Three-Dimensional X-ray Microtomography," *Science*, Vol. 237, 1987, 1439-1444.
13. D'Amico, K. L. et al., "X-ray Microtomography with Monochromatic Synchrotron Radiation" (invited), *Review of Scientific Instrument*s, Vol. 60, 1989, 1524-1526.
14. Spanne, Per and Mark L. Rivers, "Computerized Microtomography using Synchrotron Radiation from the NSLS," *Nuclear Instruments and Methods in Physics Research*, B24/25, 1987, 1063-1067.
15. Barna, S. L. et al., "Characterization of a Prototype Pixel Array Detector (PAD) for Use in Microsecond Framing Time-Resolved X-ray Diffraction Studies," *IEEE Transactions on Nuclear Science*, Vol. 44, 1997, 950-956.
16. Rossi, G. et al., "Tests of a Prototype Pixel Array Detector for Microsecond Time-Resolved X-ray Diffraction," *Journal of Synchrotron Radiation*, Vol. 6, 1999, 1096-1105.
17. Renzi, M. J. et al., "Pixel Array Detectors for Time Resolved Radiography" (invited), *Review of Scientific Instruments*, Vol. 73, 2002, 1621-1624.